Topological Nodal Cooper Pairing in Doped Weyl Metals

Yi Li and F. D. M. Haldane

Phys. Rev. Lett. **120**, 067003 — Published 9 February 2018

DOI: 10.1103/PhysRevLett.120.067003

Topological nodal Cooper pairing in doped Weyl metals

Yi Li[1] and F. D. M. Haldane[2]

[1] *Princeton Center for Theoretical Science, Princeton University, Princeton, NJ 08544, USA*
[2] *Department of Physics, Princeton University, Princeton, NJ 08544, USA*

(Dated: Dec 22, 2017)

We generalize the concept of Berry connection of the single-electron band structure to that of a two-particle Cooper pairing state between two Fermi surfaces with opposite Chern numbers. Because of underlying Fermi surface topology, the pairing Berry phase acquires non-trivial monopole structure. Consequently, pairing gap functions have topologically-protected nodal structure as vortices in the momentum space with the total vorticity solely determined by the pair monopole charge q_p. The nodes of gap function behave as the Weyl-Majorana points of the Bogoliubov-de Gennes pairing Hamiltonian. Their relation with the connection patterns of the surface modes from the Weyl band structure and the Majorana surface modes inside the pairing gap is also discussed. Under the approximation of spherical Fermi surfaces, the pairing symmetry are represented by monopole harmonic functions. The lowest possible pairing channel carries angular momentum number $j = |q_p|$, and the corresponding gap functions are holomorphic or anti-holomorphic functions on Fermi surfaces. After projected on the Fermi surfaces with non-trivial topology, all the partial-wave channels of pairing interactions acquire the monopole charge q_p independent of concrete pairing mechanism.

PACS numbers: 74.20.Rp,73.43.-f,03.65.Vf

The study of topological states has renewed our understanding of condensed matter physics. The discovery of two-dimensional integer quantum Hall states [1, 2] initiated the exploration of novel states characterized by band topology rather than symmetry [3–8], with magnetic band structures that possess non-trivial Chern numbers arising from broken time-reversal (TR) symmetry. The study of Berry curvature of Bloch bands in such lattice structures has led to rich results in anomalous Hall and quantum anomalous Hall physics [9–16]. The band structure topology has also been generalized to systems of topological insulators with TR symmetry [17–27]. The stable gapless surface modes which appear at the boundary of gapped topological systems have analogs in gapless semi-metallic systems, which can also have non-trivial band topology. For example, topological Weyl semi-metals have been proposed and realized in three-dimensional (3D) systems in the absence of either TR or inversion symmetry [28–57]. Their band structure is characterized by degenerate Weyl points in the Brillouin zone (BZ), which can be understood as monopole sources and sinks of Berry-curvature flux in $\mathbf{k}$-space.

Topological phenomena are usually understood in terms of contributions from all the filled electronic states rather than the states in the vicinity of Fermi surfaces. The apparent disagreement with the central tenet of Fermi-liquid theory that all conduction processes can be understood at the Fermi level can be resolved by introducing the Berry phase of quasi-particles on the Fermi surface [13]. So far, the study of the Fermi surface topology and the associated Berry phase structure has mainly been discussed at the single-particle level [11–14].

Here we study a novel class of exotic superconductivity which can be realized in doped Weyl metals, and more generally in systems with topologically non-trivial Fermi surfaces. In superconductivity with pairing between states on two disjoint Fermi surface sheets of opposite Chern numbers, the Cooper pair inherits a non-trivial Berry phase from their underlying topological single-particle Fermi surfaces. Consequently, the pairing gap functions develop nontrivial net vorticities leading to topologically-stable gapless nodes on the Fermi surfaces. These nodes also determine the interplay between the surface modes due to Weyl points in the band structure and those arising from Cooper pairing. For Fermi surfaces with approximately spherical symmetries, the pairing symmetry can be classified by monopole harmonic functions rather than ordinary spherical harmonics. We also performed partial-wave analysis on pairing interactions. Non-trivial Fermi surface topology transforms ordinary partial-wave channels into monopole ones characterized by the pairing monopole charge, which is determined by topology rather than concrete interactions.

We consider a general 3D electron system with a pair of separated Fermi surfaces, denoted as $\mathrm{FS}_\pm$, respectively, carrying opposite Chern numbers $\pm C$. The doped Weyl metal can be thought as a concrete example. Let us start with a minimal description that only assumes the existence of parity symmetry but broken TR symmetry. In this model, there are two Weyl points located at $\pm\mathbf{K}_0$, and are related to each other by parity and respectively surrounded by $\mathrm{FS}_\pm$. Furthermore, the parity ensures that opposite monopole charges $\pm q$ are enclosed by $\mathrm{FS}_\pm$. Define the electron creation operator $c_a^\dagger(\mathbf{k})$ in which a is the index of a general two-band structure. For the single-electron states on $\mathrm{FS}_\pm$, their creation operators are defined, respectively, as $\alpha_\pm^\dagger(\pm\mathbf{k}) = \sum_a \xi_{\pm,a}(\pm\mathbf{k}) c_a^\dagger(\pm\mathbf{K}_0 \pm \mathbf{k})$, in which $\pm\mathbf{k}$ are the relative momenta for electrons on $\mathrm{FS}_\pm$ with respect to $\pm\mathbf{K}_0$. $\xi_{\pm,a}(\pm\mathbf{k})$ are the corresponding normal-

ized eigen-functions on $\mathrm{FS}_\pm$, respectively. And $\pm\mathbf{k}$ lie on two surfaces denoted as $\mathrm{S}_\pm$ which correspond to shifting $\mathrm{FS}_\pm$ by $\mp\mathbf{K}_0$ towards the origin. Because of the non-trivial monopole structure, $\xi_{\pm,a}(\pm\mathbf{k})$ cannot be globally well-defined for $\pm\mathbf{k}$ over the entire surfaces of $\mathrm{S}_\pm$, respectively. They need to be described using a specific gauge.

The single-particle Berry connection can be defined as $\mathbf{A}_\pm(\mathbf{k}) = \sum_a \xi^*_{\pm,a}(\mathbf{k}) i\nabla_k \xi_{\pm,a}(\mathbf{k})$, in which ∇_k lies in the tangent space of $\mathrm{S}_\pm$, and, $\mathbf{A}_\pm$ is a tangent vector field therein. The Berry fluxes satisfy $\oiint_{S_\pm} d\mathbf{k}\cdot\nabla_k\times\mathbf{A}_\pm(\mathbf{k}) = \pm 4\pi q$. The simplest case of $C=1$ is associated with a fundamental monopole charge of $q=\frac{1}{2}$.

Let us consider zero-momentum inter-Fermi surface pairing between FS_+ and FS_-. The pairing operator is denoted by $P^\dagger(\mathbf{k}) = \alpha^\dagger_+(\mathbf{k})\alpha^\dagger_-(-\mathbf{k})$. As pointed out by Murakami and Nagaosa in Ref. [58], the Berry connection of the two-particle state created by $P^\dagger(\mathbf{k})$ can be expressed as $\mathbf{A}_p(\mathbf{k}) = \mathbf{A}_+(\mathbf{k}) - \mathbf{A}_-(-\mathbf{k})$. The total pairing Berry flux penetrating S_+ is $\oiint_{S_+} d\mathbf{k}\cdot\nabla_k\times\mathbf{A}_p(\mathbf{k}) = 4\pi q_p$ with $q_p = 2q$. In other words, the inter-Fermi surface Cooper pairing inherits the Berry fluxes of single electrons on topological Fermi surfaces. Consequently, the phases of Cooper pairing cannot be well-defined over the entire Fermi surfaces, which leads to generic nodal structure of pairing gap functions.

Let us consider the gap function over S_+ as $\Delta(\mathbf{k})$, which is conjugate to the pairing operator $P^\dagger(\mathbf{k})$ and is a single-valued complex function. Assuming the nodal structure of $\Delta(\mathbf{k})$ only composed of isolated points or lines, it can be proved that $\Delta(\mathbf{k})$ possesses generic nodal structure with total vorticity $2q_p$, which is a consequence of the band topology on $\mathrm{FS}_\pm$ and is independent of specific pairing mechanisms and symmetries. The gap function $\Delta(\mathbf{k})$ can be parameterized as $|\Delta(\mathbf{k})|e^{i\phi(\mathbf{k})}$, in which $\phi(\mathbf{k})$ is the pairing phase. $\Delta(\mathbf{k})$ is gauge-covariant as follows: Under the gauge transformation $\xi_\pm(\pm\mathbf{k}) \to \xi_\pm(\pm\mathbf{k})e^{i\Lambda_\pm(\pm\mathbf{k})}$, we have $\alpha^\dagger_\pm(\pm\mathbf{k}) \to \alpha^\dagger_\pm(\pm\mathbf{k})e^{i\Lambda_\pm(\pm\mathbf{k})}$, and $P^\dagger(\mathbf{k}) \to P^\dagger(\mathbf{k})e^{i\Lambda(\mathbf{k})}$ in which $\Lambda(\mathbf{k}) = \Lambda_+(\mathbf{k}) + \Lambda_-(-\mathbf{k})$. Consequently, $\phi(\mathbf{k})$ and $\mathbf{A}_p(\mathbf{k})$ transform as $\phi(\mathbf{k}) \to \phi(\mathbf{k}) - \Lambda(\mathbf{k})$ and $\mathbf{A}_p(\mathbf{k}) \to \mathbf{A}_p(\mathbf{k}) - \nabla_k\Lambda(\mathbf{k})$. We define a gauge invariant $\mathbf{k}$-space circulation field on S_+ as $\mathbf{v}(\mathbf{k}) = \nabla_k\phi(\mathbf{k}) - \mathbf{A}_p$, which is regular except at gap nodes. If we consider the case that $\Delta(\mathbf{k})$ only has isolated zeros located at $\mathbf{k}_i$ $(i = 1, 2, ..., n)$. An infinitesimally small loop C_i is defined around each gap node $\mathbf{k}_i$ with positive loop direction depending on the local normal direction by the right-hand rule. Then, $\oint_{C_i} d\mathbf{k}\cdot\mathbf{v} = 2\pi g_i$ in which g_i is the vorticity and integer valued. Next, reversing the direction of each loop C_i and applying Stokes' theorem on S_+ (excluding the bad points $\mathbf{k}_i$'s on which $\mathbf{v}$ is ill-defined), we arrive at

$$\sum_i g_i = \sum_i \oint_{C_i} \frac{d\mathbf{k}}{2\pi}\cdot\mathbf{v} = \oiint \frac{d\mathbf{k}}{2\pi}\cdot(\nabla_k\times\mathbf{A}_p) = 2q_p. \quad (1)$$

This proof is gauge-independent. If $\Delta(\mathbf{k})$ has line-nodes on S_+ which behave as branch-cuts of $\mathbf{v}$, the proof can also be done similarly.

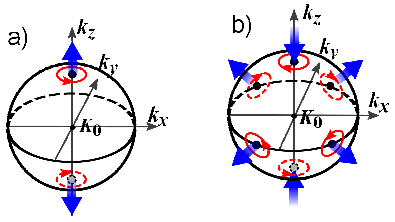

FIG. 1. Two possible nodal structures of gap functions $\Delta(\mathbf{k})$ on a Fermi surface S_+ for $q_p = 1$. Both nodes at the north and south poles are vortices of the pairing phase with vorticity $+1$ for a) when $\Delta_y = -i\Delta_x$ and anti-vortices with vorticity -1 for b) when $\Delta_y = i\Delta_x$. Each node in the equator plane in b), exhibits vorticity $+1$. The total vorticity is $2q_p$ for both.

Consequently, when $q_p \neq 0$, $\Delta(\mathbf{k})$ cannot be a regular function over the entire S_+. Its nodal structure is distinct from that of the usual pairing symmetry based on spherical harmonics $Y_{lm}(\hat{\mathbf{k}})$, which are regular functions over a sphere. The absence of the monopole structure gives rise to vanishing total vorticity of phases. For example, for ^{3}He-A type pairing with orbital symmetry $Y_{11}(\hat{\mathbf{k}})$, two nodes at the north and south poles are a vortex and an anti-vortex of the pairing phases, respectively.

To illustrate this, we use a modified Rice-Mele model [59] describing 3D Weyl semi-metals in an array of bipartite lattice A and B planes with spinless fermions [35, 43],

$$H_K = \sum_{a,b=A,B}\sum_{\mathbf{k}} c^\dagger_a(\mathbf{k})\big\{[t_- + t_+\cos(2k_x)]\sigma_x + \\ +t_+\sin(2k_x)\sigma_y + V\sigma_z - \mu\big\}_{ab} c_b(\mathbf{k}), \quad (2)$$

in which the eigenbasis of σ_z refer to A B sublattices, $t_+ = 1$, $t_- = -(k_y^2 + k_z^2)$, and $V = 2k_y$. H_K is invariant under inversion with respect to the center of a bond along x-direction, *i.e.*, $A \leftrightarrow B$, $\mathbf{k} \to -\mathbf{k}$, but breaks TR symmetry under which $\sigma_y \to -\sigma_y$ and $\mathbf{k} \to -\mathbf{k}$. This model has additional symmetries, including a mirror symmetry M_{xy}, $k_z \to -k_z$, and a combined TR with mirror M_{xz}, $k_y \to -k_y$ (or M_{yz}, $A \leftrightarrow B$, $k_x \to -k_x$) symmetry. If $\mu > 0$, the Fermi surfaces $\mathrm{FS}_\pm$ enclosing $\pm\mathbf{K}_0$ have Chern numbers $C = \pm 1$, respectively.

Consider the following pairing Hamiltonian

$$H_\Delta = \sum_{a,b;\mathbf{k}} c^\dagger_a(\mathbf{k}) 2i[\Delta_x\sin(2k_x) + \Delta_y\sin k_y\sigma_x]_{ab} c^\dagger_b(-\mathbf{k}) \\ + h.c. \quad (3)$$

The corresponding tight-binding model is presented in the Suppl. Mat. A [60]. Assuming that the system is in a weak pairing region, *i.e.*, $|\Delta_{x,y}| \ll |\mu|$, we can project the pairing onto $\mathrm{FS}_\pm$. Since the gap function satisfies $\Delta(-\mathbf{k}) = -\Delta(\mathbf{k})$, let's consider $\Delta(\mathbf{k})$ on FS_+ only. $\Delta(\mathbf{k})$ exhibits two nodes at the north and south poles of FS_+. We choose two different gauges, which are respectively

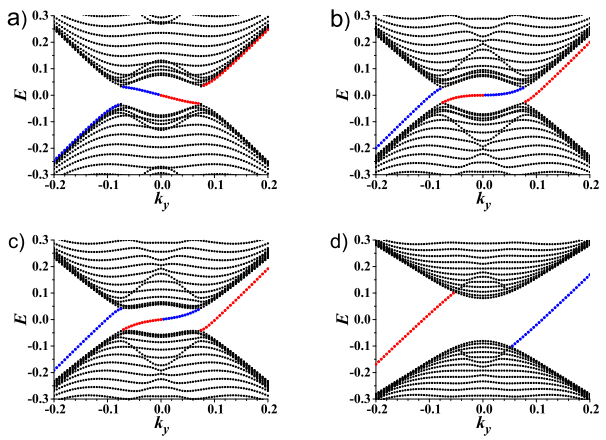

FIG. 2. (Color Online) Bulk and surface spectra (for a single open boundary in the yz-plane) vs. k_y at different values of $k_z = 1.03, 0.95, 0.93, 0.85$ for a) to d). The parameters are $\mu = 0.2$ and $\Delta_y = i\Delta_x$ with $\Delta_x = 0.2$. Red (Blue) points represent surface modes with positive (negative) charges.

non-singular in the two polar regions. Then, the gap function can be approximated as $\Delta(\mathbf{k}) = \mp\Delta_x k_x + \Delta_y k_y$ at the north and south poles, respectively. If $\Delta_y = -i\Delta_x$, the circulation field $\mathbf{v}(\mathbf{k})$ exhibits a pair of vortices located at the north and south poles with vorticity $+1$ (Fig. 1 a)). There are no other nodes on FS_+, and the total vorticity is $+2$ in agreement with Eq. (1). In contrast, if $\Delta_y = i\Delta_x$, the nodes at the north and south poles change their vorticity to -1. However, the total vorticity on FS_+ remains $+2$ which implies additional nodes. In our model, four additional nodes are found on the equator with azimuthal angles $\pm\frac{\pi}{4}$ and $\pm\frac{3\pi}{4}$ and with vorticity $+1$ each (Fig. 1 b)).

Next, we study surface spectra under open boundary conditions. In the absence of pairing, it is well-known that surface Fermi arc states are formed by in-gap chiral states for k_z between two bulk Weyl points with $|k_z| < K_{0,z}$ [29, 31, 43]. When superconductivity opens pairing gaps on $\mathrm{FS}_\pm$, additional surface Majorana modes can be generated inside the gap. Specific locations of these Majorana modes are determined by the pairing nodes on $\mathrm{FS}_\pm$ and the associated vorticity pattern. As have been described in Ref. [54], in the presence of a combined time-reversal and mirror reflection with respect to the plane bisecting a bond along x here, surface Majorana states must connect to surface Fermi arcs arising from the Weyl band structure as k_z varies.

We impose two open boundaries parallel to the yz-plane, and plot the spectra vs. k_y at different values of k_z, with modes localized on the bottom boundary suppressed. The results of the case $\Delta_y = i\Delta_x$ are shown in Fig. 2 a)-d), and those of $\Delta_y = -i\Delta_x$ are presented in Suppl. Mat. B [60]. Because of the mirror symmetry, the spectrum is invariant under $k_z \mapsto -k_z$ together with a particle-hole transformation. At $\mu = 0.2$, FS_+ enclosing $K_0 = (0, 0, 1)$ intersects the k_z-axis at $k_n \approx 1.1$ (the north pole) and $k_s \approx 0.9$ (the south pole). For cuts at $k_z > k_n$, or, $k_z < k_s$, since they do not intersect FS_+, the corresponding surface spectra are determined by the Weyl band structure: No surface modes exist at $k_z > k_n$; but two branches of chiral surface modes appear at $-k_s < k_z < k_s$ (Fig. 2 d)) which are related by the particle-hole transformation, which reverses their charges and maps $(k_y, k_z) \mapsto (-k_y, -k_z)$, followed by a z-reflection, $(-k_y, -k_z) \mapsto (-k_y, k_z)$. Consequently, for fixed $-k_s < k_z < k_s$ one surface mode is electron-like (the standard Fermi arc) with a quasiparticle charge $0 < e^*(k_y, k_z) < e$, and the other is the z-reflection of its particle-hole conjugate, with $e^*(-k_y, k_z) < 0$. Because k_z lies outside $\mathrm{FS}_\pm$, the particle-hole mixing is weak, so the charge of the electron-like arc mode is close to e.

As k_z crosses the Fermi surface FS_+ , each k_z defines a Fermi-surface cross section (FS-CS) on FS_+ of the Weyl metal, which becomes gapped by pairing. The surface band topology changes when k_z passes gap closing points, which are the zero energy Weyl-Majorana (WM) points for the bulk BdG Hamiltonian. These WM points are classified as positive or negative according to their chiral indices. As shown in Fig. 1 b), the WM points at the north and the south poles are negative; while those near the equator are positive. As k_z decreases through the WM point at the north pole, the surface gap closes and reopens. Within the FS-CS, a single surface mode with negative chirality passing through zero energy as shown in Fig. 2 a). The gap closes again at $k_z \approx K_0$, where projections of the four positive WM points are found. As the cut of k_z further moves downward, the gap reopens and there are three surface modes with positive chirality (Fig. 2 b) and c)). The central zero-energy mode inside the FS-CS is mostly of the Majorana nature arising from pairing but its chirality is opposite to that in Fig. 2 a). The other two mostly arise from the Weyl band structure. After k_z passes the WM point at the south pole which contributes vorticity -1, the number of surface modes is decreased to two (Fig. 2 d)), as BdG doubled usual Fermi arcs in Weyl semi-metals.

When $k_n > k_z > k_s$, the charge of surface quasiparticles changes continuously as a function of k_y from hole-like to particle-like through a "neutral point", which in our model is pinned at $k_y = 0$ by the z-reflection symmetry $e^*(k_y, k_z) \equiv -e^*(-k_y, -k_z) = e^*(-k_y, k_z)$. In general, these points form a "neutrality line" in the surface BZ connecting the projections of the two WM points. The z-reflection symmetry also gives the quasi-particle spectrum the symmetry $E(k_y, k_z) \equiv -E(-k_y, -k_z) = E(-k_y, k_z)$, so the zero-energy line, like the neutral point is pinned to $k_y = 0$, and its group velocity is in the y-direction. Near the north pole, the zero-energy point has group-velocity in the $-\hat{y}$ direction, while near the south pole, it is along $+\hat{y}$. A consequence of the reflection sym-

metry is that at some intermediate k_z, its group velocity vanishes.

Next we study the pairing partial-wave symmetries when $\mathrm{FS}_\pm$ have approximate spherical symmetry. If we neglect the small anisotropy, the complete bases of $\Delta(\mathbf{k})$ for $\mathbf{k}$ lying on S_+ with a total vorticity $2q_p$ are spanned by monopole harmonic functions $Y_{q_p,jm}(\hat{\mathbf{k}})$ instead of spherical harmonics Y_{lm}. Monopole harmonic functions have been widely applied in physics [4, 61, 62]. For completeness, their basic properties are summarized in Suppl. Mat. C [60]. After projecting to $\mathrm{FS}_\pm$, the pairing Hamiltonian becomes $H_\Delta = \sum_{\mathbf{k}} \Delta(\mathbf{k}) P^\dagger(\mathbf{k}) + \Delta^*(\mathbf{k}) P(\mathbf{k})$ for $\mathbf{k}$ lying close to S_+. We define $\Delta(\mathbf{k}) = \Delta(|k|) f(\hat{\mathbf{k}})$, in which the angular dependence on $\hat{\mathbf{k}}$ and the energy dependence on $|k|$ are separated. $\Delta(|k|)$ is assumed positive and the angular factor $f(\hat{k})$ is complex satisfying the normalization condition $\int d\hat{\mathbf{k}} |f(\hat{k})|^2 = 1$. $f(\hat{\mathbf{k}})$ is expanded in terms of the monopole harmonic functions as

$$f(\hat{\mathbf{k}}) = \sum_{jm} c_{jm} \mathcal{Y}_{q_p;jm}(\hat{\mathbf{k}}), \tag{4}$$

in which c_{jm} are complex coefficients. Both the pairing operator $P^\dagger(\mathbf{k})$ and the gap function $\Delta(\mathbf{k})$ are gauge dependent, while, H_Δ is gauge independent.

A remarkable feature is that all the pairing channels should follow $j \geq |q_p|$ regardless of the pairing mechanism since $\mathcal{Y}_{q_p,j,m}$ starts from $j = |q_p|$. The absence of pairing channels with $j < |q_p|$ is robust as a consequence of topology and the monopole harmonic representation of a rotation group. Furthermore, the lowest order pairing channel $j = |q_p|$ is special: $\mathcal{Y}_{q_p,j=|q_p|,m}(\hat{\mathbf{k}})$ are holomorphic or anti-holomorphic functions. All of its $2q_p$-nodes exhibit the same vorticity, and thus $\Delta(\mathbf{k})$ is completely determined by the locations of its nodes up to an overall factor. The nodes of $\mathcal{Y}_{q_p,j=|q_p|,m}(\hat{\mathbf{k}})$ represent vortices of the pairing phases on S_+. The location of pairing nodes are also WM points of the BdG Hamiltonian with the same chirality. For each node on FS_+ at $\mathbf{K}_0 + \mathbf{k}$, there exists its image on FS_- exhibiting the opposite vorticity. In the Suppl. Mat. D [60], we use concrete examples to further illustrate the distribution of pairing nodes on the approximately spherical Fermi surface.

We next perform partial-wave analysis of the pairing interactions. It is the non-trivial topology of $\mathrm{FS}_\pm$ that transforms the ordinary partial-wave channels into those characterized by monopole harmonics starting with $j = |q_p|$, which is in fact independent of concrete pairing mechanism. For simplicity, we consider a concrete example: The low energy band Hamiltonians around the Weyl points $\pm\mathbf{K}_0$ as $H_{w,\pm}(\pm\mathbf{K}_0 + \mathbf{k}) = \pm v\sigma \cdot \mathbf{k} - \mu$, where σ's represent Pauli matrices for spins, and, without loss of generality, $\mu > 0$ is assumed. Due to the opposite chiralities of $\mathrm{FS}_\pm$, the inter-Fermi surface Cooper pairing is between two electrons with parallel spins. Hence, only the spin triplet pairing channel is considered, expressed as $H_{pair} = \sum_{\mathbf{k},\mathbf{k}';m} V_t(\mathbf{k},\mathbf{k}') \chi^\dagger_{1m}(\mathbf{k}) \chi_{1m}(\mathbf{k}') + h.c.$, where $\chi^\dagger_{1m}(\mathbf{k}) = \sum_{\sigma\sigma'} \langle 1m|\frac{1}{2}\sigma;\frac{1}{2}\sigma'\rangle c^\dagger_\sigma(\mathbf{K}_0 + \mathbf{k}) c^\dagger_{\sigma'}(-\mathbf{K}_0 - \mathbf{k})$. are the spin triplet pairing operators. Since usual interactions in solids do not directly flip spins, the spin index m is expressed in the S_z-eigenbasis. So far, H_{pair} has not been expressed in the helical basis, and hence it is still *not* the low energy pairing Hamiltonian. To project H_{pair} to helical Fermi surfaces, the pairing operator on $\mathrm{FS}_\pm$ is expressed as $P(\mathbf{k}) = \sqrt{\frac{4\pi}{3}} \sum_{m=-1}^{1} Y_{-1;1m}(\hat{\mathbf{k}}) \chi_{1m}(\mathbf{k})$, and the consequential projected pairing Hamiltonian is

$$\tilde{H}_{pair} = \sum_{\mathbf{k},\mathbf{k}' \in \mathrm{S}_+} \tilde{V}(\mathbf{k},\mathbf{k}') P^\dagger(\mathbf{k}) P(\mathbf{k}') + h.c., \tag{5}$$

in which $\mathbf{k}$ and $\mathbf{k}'$ are on S_+ , and,

$$\tilde{V}(\mathbf{k},\mathbf{k}') = \frac{4\pi}{3} Y^*_{-1;1m}(\hat{\mathbf{k}}) V_t(\mathbf{k},\mathbf{k}') Y_{-1;1,m}(\hat{\mathbf{k}}'), \tag{6}$$

is the projected pair scattering matrix element. Because of Fermi statistics, the pair scattering matrix element before projection is expressed as $V_t(\mathbf{k},\mathbf{k}') = V(\mathbf{k} - \mathbf{k}') - V(\mathbf{k} + \mathbf{k}' + 2\mathbf{K}_0)$, where the first and second terms are the intra- and inter-Fermi surface scattering, respectively. The inter-Fermi surface scattering involves large momentum transfer and will be neglected below. As for the intra-Fermi surface scattering $V(\mathbf{k} - \mathbf{k}')$, for simplicity, we assume it is factorizable and rotationally invariant around K_0 for $\mathbf{k}$ and $\mathbf{k}'$ on S_+, such that it only depends on the relative angle between $\mathbf{k}$ and $\mathbf{k}'$ as $V(\mathbf{k}-\mathbf{k}') = V(\hat{\mathbf{k}}\cdot\hat{\mathbf{k}}')$. Unlike the usual case, i.e., $\mathbf{K}_0 = 0$, that V_t only contains the odd partial-wave channels, here, both even and odd partial-wave channels are allowed as $V_t(\mathbf{k},\mathbf{k}') = V(\hat{\mathbf{k}}\cdot\hat{\mathbf{k}}') = \sum_{lm} \frac{4\pi g_l}{2l+1} Y^*_{lm}(\hat{\mathbf{k}}) Y_{lm}(\hat{\mathbf{k}})$ in which l is integer-valued.

After the projection, as defined in Eq. (6), pairing interaction becomes

$$\tilde{V}(\hat{\mathbf{k}}\cdot\hat{\mathbf{k}}') = \sum_{j\geq 1,m} \tilde{g}_j Y^*_{-1,jm}(\hat{\mathbf{k}}') Y_{1,jm}(\hat{\mathbf{k}}), \tag{7}$$

with $\tilde{g}_j = \frac{1}{2j+1} \sum_{l=j,j\pm1} (2l+1) g_l |\langle l0;11|j1\rangle|^2$. The monopole harmonic partial wave channels start from $j = 1$. In other words, the projection to helical Fermi surfaces reorganizes all partial-wave channels and shifts the lowest partial wave channel from $j = 0$ to 1. The actual pairing channel that the system prefers is determined by where the most negative eigenvalue lies in the pairing matrix.

In summary, we have studied the Cooper pairing symmetry between two separate Fermi surfaces carrying opposite Chern numbers $\pm C$. The Cooper pairs carry a non-trivial Berry phase structure characterized by the monopole charge $q_p = C$ so that their phases cannot be globally well-defined on the Fermi surfaces. The gap function $\Delta(\mathbf{k})$ generically possesses nodes with the total vorticity $2q_p$. These nodes are also the WM points of the Hamiltonian in the BdG formalism. The surface modes

arise both from the Weyl band structure and the pairing: the former exist inside the band gap, while the latter appear inside the pairing gap on $FS_{\pm}$. In a simplified model where $FS_{\pm}$ are both spherical, the pairing symmetry is classified in terms of the monopole harmonic functions. The lowest pairing channel is $j = |q_p|$ which is purely determined by topology rather than interactions. The corresponding pairing functions are holomorphic or anti-holomorphic functions on the pairing surface. Partial-wave analysis shows that the ordinary pairing interactions, when projected on these topologically non-trivial Fermi surfaces, acquired the pairing monopole charge in all the partial wave channels regardless of concrete pairing mechanism.

Y. L. thanks N.P. Ong and C. Wu for consistent encouragement on this project and the Princeton Center for Theoretical Science at Princeton University for support. F.D.M.H. was supported in part by the MRSEC program at Princeton Center for Complex Materials, grant NSF-DMR-1420541, and by the W. M. Keck Foundation.

[1] K. v. Klitzing, G. Dorda, and M. Pepper, Phys. Rev. Lett. **45**, 494 (1980).
[2] D. C. Tsui, H. L. Stormer, and A. C. Gossard, Phys. Rev. Lett. **48**, 1559 (1982).
[3] D. J. Thouless, M. Kohmoto, M. P. Nightingale, and M. den Nijs, Phys. Rev. Lett. **49**, 405 (1982).
[4] F. D. M. Haldane, Phys. Rev. Lett. **51**, 605 (1983).
[5] J. E. Avron, R. Seiler, and B. Simon, Phys. Rev. Lett. **51**, 51 (1983).
[6] Q. Niu, D. Thouless, and Y. Wu, Phys. Rev. B **31**, 3372 (1985).
[7] M. Kohmoto, Ann. Phys. **160**, 343 (1985).
[8] J. E. Avron, R. Seiler, and B. Simon, Phys. Rev. Lett. **65**, 2185 (1990).
[9] F. D. M. Haldane, Phys. Rev. Lett. **61**, 2015 (1988).
[10] R. Karplus and J. M. Luttinger, Phys. Rev. **95**, 1154 (1954).
[11] T. Jungwirth, Q. Niu, and A. H. MacDonald, Phys. Rev. Lett. **88**, 207208 (2002).
[12] M. Onoda and N. Nagaosa, J. Phys. Soc. Jpn. **71**, 19 (2002).
[13] F. D. M. Haldane, Phys. Rev. Lett. **93**, 206602 (2004).
[14] N. Nagaosa, J. Sinova, S. Onoda, A. H. MacDonald, and N. P. Ong, Rev. Mod. Phys. **82**, 1539 (2010).
[15] R. Yu, W. Zhang, H.-J. Zhang, S.-C. Zhang, X. Dai, and Z. Fang, Science **329**, 61 (2010).
[16] C.-Z. Chang, J. Zhang, X. Feng, J. Shen, Z. Zhang, M. Guo, K. Li, Y. Ou, P. Wei, L.-L. Wang, Z.-Q. Ji, Y. Feng, S. Ji, X. Chen, J. Jia, X. Dai, Z. Fang, S.-C. Zhang, K. He, Y. Wang, L. Lu, X.-C. Ma, and Q.-K. Xue, Science **340**, 167 (2013).
[17] C. L. Kane and E. J. Mele, Phys. Rev. Lett. **95**, 226801 (2005).
[18] C. L. Kane and E. J. Mele, Phys. Rev. Lett. **95**, 146802 (2005).
[19] B. A. Bernevig and S.-C. Zhang, Phys. Rev. Lett. **96**, 106802 (2006).
[20] B. A. Bernevig, T. L. Hughes, and S.-C. Zhang, Science **314**, 1757 (2006).
[21] L. Fu and C. L. Kane, Phys. Rev. B **76**, 045302 (2007).
[22] L. Fu, C. L. Kane, and E. J. Mele, Phys. Rev. Lett. **98**, 106803 (2007).
[23] J. E. Moore and L. Balents, Phys. Rev. B **75**, 121306 (2007).
[24] X.-L. Qi, T. L. Hughes, and S.-C. Zhang, Phys. Rev. B **78**, 195424 (2008).
[25] R. Roy, Phys. Rev. B **79**, 195322 (2009).
[26] M. Z. Hasan and C. L. Kane, Rev. Mod. Phys. **82**, 3045 (2010).
[27] X.-L. Qi and S.-C. Zhang, Rev. Mod. Phys. **83**, 1057 (2011).
[28] S. Murakami, New J. Phys. **9**, 356 (2007).
[29] X. Wan, A. M. Turner, A. Vishwanath, and S. Y. Savrasov, Phys. Rev. B **83**, 205101 (2011).
[30] A. A. Burkov and L. Balents, Phys. Rev. Lett. **107**, 127205 (2011).
[31] K.-Y. Yang, Y.-M. Lu, and Y. Ran, Phys. Rev. B **84**, 075129 (2011).
[32] T. Meng and L. Balents, Phys. Rev. B **86**, 054504 (2012).
[33] W. Witczak-Krempa and Y. B. Kim, Phys. Rev. B **85**, 045124 (2012).
[34] G. Y. Cho, J. H. Bardarson, Y.-M. Lu, and J. E. Moore, Phys. Rev. B **86**, 214514 (2012).
[35] P. Hosur, Phys. Rev. B **86**, 195102 (2012).
[36] C. Fang, M. J. Gilbert, X. Dai, and B. A. Bernevig, Phys. Rev. Lett. **108**, 266802 (2012).
[37] D. T. Son and B. Z. Spivak, Phys. Rev. B **88**, 104412 (2013).
[38] P. Hosur and X. Qi, C. R. Phys. **14**, 857 (2013), arXiv:1309.4464 [cond-mat.str-el].
[39] M. Vazifeh and M. Franz, Phys. Rev. Lett. **111**, 027201 (2013).
[40] P. Hosur, X. Dai, Z. Fang, and X.-L. Qi, Phys. Rev. B **90**, 045130 (2014).
[41] S. A. Yang, H. Pan, and F. Zhang, Phys. Rev. Lett. **113**, 046401 (2014).
[42] A. C. Potter, I. Kimchi, and A. Vishwanath, Nat. Commun. **5**, 5161 (2014).
[43] F. D. M. Haldane, ArXiv e-prints (2014), arXiv:1401.0529 [cond-mat.str-el].
[44] H. Wei, S.-P. Chao, and V. Aji, Phys. Rev. B **89**, 014506 (2014).
[45] R. Nandkishore, D. A. Huse, and S. L. Sondhi, Phys. Rev. B **89**, 245110 (2014).
[46] H. Weng, C. Fang, Z. Fang, B. A. Bernevig, and X. Dai, Phys. Rev. X **5**, 011029 (2015).
[47] A. A. Burkov, J. Phys.: Condens. Matter **27**, 113201 (2015).
[48] S.-Y. Xu, N. Alidoust, I. Belopolski, Z. Yuan, G. Bian, T.-R. Chang, H. Zheng, V. N. Strocov, D. S. Sanchez, G. Chang, C. Zhang, D. Mou, Y. Wu, L. Huang, C.-C. Lee, S.-M. Huang, B. Wang, A. Bansil, H.-T. Jeng, T. Neupert, A. Kaminski, H. Lin, S. Jia, and Z. M. Hasan, Nature Phys. **11**, 748 (2015).
[49] S.-Y. Xu, I. Belopolski, N. Alidoust, M. Neupane, G. Bian, C. Zhang, R. Sankar, G. Chang, Z. Yuan, C.-C. Lee, S.-M. Huang, H. Zheng, J. Ma, D. S. Sanchez, B. Wang, A. Bansil, F. Chou, P. P. Shibayev, H. Lin, S. Jia, and M. Z. Hasan, Science **349**, 613 (2015).
[50] B. Q. Lv, H. M. Weng, B. B. Fu, X. P. Wang, H. Miao, J. Ma, P. Richard, X. C. Huang, L. X. Zhao,

G. F. Chen, Z. Fang, X. Dai, T. Qian, and H. Ding, Phys. Rev. X **5**, 031013 (2015).
[51] B. Q. Lv, N. Xu, H. M. Weng, J. Z. Ma, P. Richard, X. C. Huang, L. X. Zhao, G. F. Chen, C. Matt, F. Bisti, V. Strokov, J. Mesot, Z. Fang, X. Dai, T. Qian, M. Shi, and H. Ding, Nature Phys. **11**, 724 (2015).
[52] G. Bednik, A. A. Zyuzin, and A. A. Burkov, ArXiv e-prints (2015), arXiv:1506.05109 [cond-mat.str-el].
[53] S.-K. Jian, Y.-F. Jiang, and H. Yao, Phys. Rev. Lett. **114**, 237001 (2015).
[54] B. Lu, K. Yada, M. Sato, and Y. Tanaka, Phys. Rev. Lett. **114**, 096804 (2015).
[55] S. Borisenko, D. Evtushinsky, Q. Gibson, A. Yaresko, T. Kim, M. Ali, B. Buechner, M. Hoesch, and R. J. Cava, arXiv preprint arXiv:1507.04847 (2015).
[56] Y. Qi, P. G. Naumov, M. N. Ali, C. R. Rajamathi, O. Barkalov, Y. Sun, C. Shekhar, S.-C. Wu, V. Süß, M. Schmidt, E. Pippel, P. Werner, R. Hillebrand, T. Förster, E. Kampertt, W. Schnelle, S. Parkin, R. J. Cava, C. Felser, B. Yan, and S. A. Medvedev, ArXiv e-prints (2015), arXiv:1508.03502 [cond-mat.mtrl-sci].
[57] J. Xiong, S. K. Kushwaha, T. Liang, J. W. Krizan, M. Hirschberger, W. Wang, R. Cava, and N. Ong, Science **350**, 413 (2015).
[58] S. Murakami and N. Nagaosa, Phys. Rev. Lett. **90**, 057002 (2003).
[59] M. J. Rice and E. J. Mele, Phys. Rev. Lett. **49**, 1455 (1982).
[60] See Supplemental Material for explanations and technical details, which includes Refs. [63-66].
[61] T. T. Wu and C. N. Yang, Nucl. Phys. B **107**, 365 (1976).
[62] T. T. Wu and C. N. Yang, Phys. Rev. D **16**, 1018 (1977).
[63] Y. Li and C. Wu, Scientific Reports **2**, 392 (2012).
[64] A. Larkin and Y. N. Ovchinnikov, Zh. Eksperim. i Teor. Fiz. **47** (1964).
[65] P. Fulde and R. A. Ferrell, Phys. Rev. **135**, A550 (1964).
[66] X.-L. Qi, T. L. Hughes, and S.-C. Zhang, Phys. Rev. B **81**, 134508 (2010)
.